ACS OMEGA

Article

Cite This: ACS Omega 2018, 3, 6506−6512

# Catalytic Ozonation for the Degradation of 5-Sulfosalicylic Acid with Spinel-Type $ZnAl_2O_4$ Prepared by Hydrothermal, Sol−Gel, and Coprecipitation Methods: A Comparison Study

Qizhou Dai,*[,†] Zhuo Zhang,[†] Tingting Zhan,[†] Zhong-Ting Hu,[†] and Jianmeng Chen*[,‡]

[†]College of Environment and [‡]Key Laboratory of Microbial Technology for Industrial Pollution Control of Zhejiang Province, Zhejiang University of Technology, Hangzhou 310032, China

**ABSTRACT:** This study presents a novel spinel-type zinc aluminate nanometer catalyst and is applied in catalytic ozonation for wastewater treatment. The zinc aluminate ($ZnAl_2O_4$) catalysts were synthesized by hydrothermal, sol−gel, and coprecipitation methods, and their characteristics were analyzed by X-ray diffraction, transmission electron microscopy, energy-dispersive X-ray spectrum, Fourier transform infrared, and X-ray photoelectron spectroscopy (XPS) techniques. 5-Sulfosalicylic acid (SSal) was selected as the typical pharmaceutical and personal care product and used to evaluate the catalytic activity of $ZnAl_2O_4$. Compared to ozonation, an obviously higher removal efficiency for the SSal degradation was achieved with the nanocatalyst addition in catalytic ozonation. The removal of SSal and chemical oxygen demand reached 64.8 and 46.2%, respectively, after 60 min in the presence of $ZnAl_2O_4$, whereas it was only 49.4 and 33.2%, respectively, in ozonation. The comparison of catalysts showed that the $ZnAl_2O_4$ prepared by the hydrothermal method presented a better catalytic activity in ozonation. The effect of radical scavenger experiment results and the characterization of XPS implied that •OH was the main active oxidative species in catalytic ozonation. The reusability results showed that the $ZnAl_2O_4$ catalyst possessed a high stability and could be widely used in catalytic ozonation for wastewater treatment.

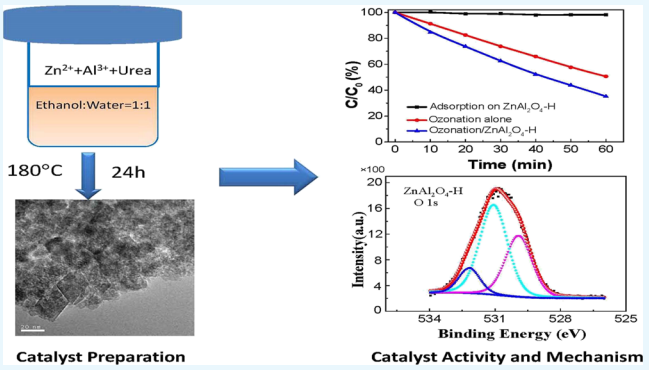


## 1. INTRODUCTION

The pharmaceutical and personal care products (PPCPs) are widespread in aquatic environments, and the pollution of PPCPs has received much attention by the environmental workers. 5-Sulfosalicylic acid (SSal) is a typical PPCP and widely used as the medical intermediate and fine chemical material.[1] Because of the poor chemical oxidability and biodegradability, the industrial wastewater containing SSal is difficult to be treated by the conventional biological system. Thus, the effective removal of SSal from wastewater has a significant impact on the environment.

In recent decades, advanced oxidation processes (AOPs) such as ozonation, electrooxidation, photooxidation, and Fenton have been intensively investigated.[2−6] AOPs could deal with organic pollutants in water through the formation of •OH (redox potential = 2.8 V ev, SHE), which could react rapidly and nonselectively with nearly all types of organic compounds.[7−9] As one of the AOPs, ozonation has been widely applied in wastewater treatment for its strong oxidizing, simple operation, and environmental friendly properties.[10] In general, organics degradation by ozonation includes two pathways: direct molecular ozone oxidation and indirect reaction via the decomposition of ozone to generate the hydroxyl radicals (•OH) to attack target pollutants. The direct oxidation with ozone is relatively slow and selective, so it could not remove the pollutants completely, especially some refractory organic compounds.[11] Also, direct ozonation may require higher energy and cost in water treatment.[12,13] Therefore, catalytic ozonation through indirect oxidation reaction has received considerable research attention.

As compared to homogeneous catalytic ozonation, heterogeneous catalytic ozonation could recycle the catalyst from the reaction solution without producing secondary pollution with solid catalysts, such as metal oxides (e.g., $Al_2O_3$, $MnO_2$, $CeO_2$, and $TiO_2$) or supported metal oxides (e.g., Ni/$CeO_2$, Co/$Al_2O_3$, and $TiO_2/Al_2O_3$).[12,14,15] Compared with other conventional catalysts, $ZnAl_2O_4$ is considered to be a promising ozonation catalyst with the advantages of being nontoxic and inexpensive and possessing good diffusion, high thermal stability, excellent activity, and relatively wide surface area.[16−19] These characteristics make it very suitable for the application.

In this work, the $ZnAl_2O_4$ catalyst was prepared by hydrothermal, sol−gel, and coprecipitation methods and used in catalytic ozonation of wastewater. SSal was selected as the model pollutant to explore the catalytic performance of three

Received: February 13, 2018
Accepted: May 11, 2018
Published: June 18, 2018

  

DOI: 10.1021/acsomega.8b00263
ACS Omega 2018, 3, 6506−6512

different catalysts. The crystal structure, texture, morphology, size, and chemical form of the surface element and the atomic ratio of catalysts were characterized by X-ray diffraction (XRD), transmission electron microscopy (TEM), energy-dispersive X-ray spectrum (EDX), Fourier transform infrared (FT-IR), and X-ray photoelectron spectroscopy (XPS). In addition, the stability and reusability of the $ZnAl_2O_4$ catalyst was also discussed.

## 2. RESULTS AND DISCUSSION

**2.1. Characterization of $ZnAl_2O_4$.** The crystallization phases of prepared catalysts were identified by XRD, which are presented in Figure 1. $ZnAl_2O_4$−C, $ZnAl_2O_4$−S, and $ZnAl_2O_4$−H exhibited the characteristic XRD peaks corresponding to (2 2 0), (3 1 1), (4 0 0), (3 3 1), (4 2 2), (5 1 1), (4 4 0), (6 2 0), and (5 3 3) planes reflection of $ZnAl_2O_4$ with a spinel cubic structure (JCPDS no. 05-0669). No impurity phases were observed. After comparison of the three catalysts, the diffraction peaks of $ZnAl_2O_4$−S were more intensive and sharper, which demonstrated higher crystallization. On the other hand, the wider peaks of $ZnAl_2O_4$−C indicated its smaller particle size. On the basis of Scherrer's formula,[20] the average crystallite sizes of $ZnAl_2O_4$−C, $ZnAl_2O_4$−H, and $ZnAl_2O_4$−S were calculated to be ca. 12, 14, and 25.3 nm, respectively, by full width at half-maximum intensity of the (3 1 1) plane of the $ZnAl_2O_4$ phase.

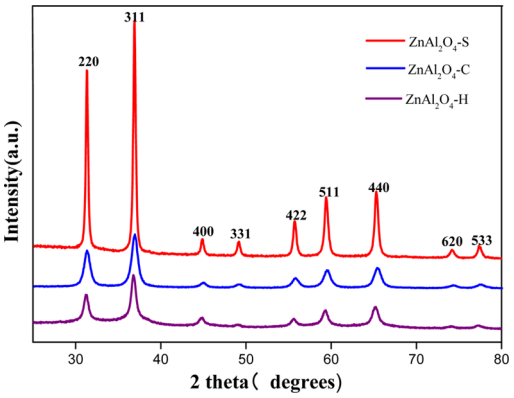


**Figure 1.** XRD patterns of $ZnAl_2O_4$ samples.

TEM and selected area electron diffraction (SAED) analysis are effective methods to identify the morphologies of the catalyst, whose results are in good accordance with XRD results.[21] Figure 2a−d showed the TEM micrographs of $ZnAl_2O_4$. It could be seen that the particle size distribution of three catalysts was very narrow, and the size was measured by a digital micrograph.[22] The nanoparticle sizes of $ZnAl_2O_4$−C, $ZnAl_2O_4$−H, and $ZnAl_2O_4$−S varied from 11−14, 14−23, and 18−28 nm, respectively. A high-resolution TEM micrograph (inset in Figure 2d) of $ZnAl_2O_4$−H showed a lattice fringe of distance of about 0.247 nm corresponding to the (3 1 1) plane of the cubic zinc aluminate structure from XRD. Furthermore, the SAED pattern, presented in Figure 2e, exhibits the diffraction rings with *d*-spacings about 0.284, 0.247, 0.203, 0.156, and 0.142 nm, which are assigned to (220), (311), (400), (511), and (440) planes of the spinel phase, respectively. The same conclusion was drawn from $ZnAl_2O_4$−C and $ZnAl_2O_4$−S. EDX was used to analyze the element or chemical characterization of the catalyst qualitatively.[10] Figure 2f gave the EDX pattern of $ZnAl_2O_4$ samples. Clearly, the prepared catalyst samples were composed of Zn, Al, and O.

The $pH_{pzc}$ could be used to determine the catalytic property. In this work, we obtained the $pH_{pzc}$ by the pH drift method. When pH < $pH_{pzc}$, the hydroxyls groups at the surface of the catalyst become protonated and has a positive charge. On the contrary, when pH > $pH_{pzc}$, the hydroxyl groups at the surface of the catalytic become deprotonated and have a negative charge. From Figure 3, the $pH_{pzc}$ values of 8.00, 7.13, and 7.00 for $ZnAl_2O_4$−H, $ZnAl_2O_4$−S, and $ZnAl_2O_4$−C were obtained, respectively. The surface hydroxyl groups were analyzed, which could promote the generation of $^{\bullet}OH$ from aqueous ozone.[23] For $ZnAl_2O_4$−H, $ZnAl_2O_4$−S, and $ZnAl_2O_4$−C, the densities of surface hydroxyl groups were 3.2, 2.5, and 2.3 mmol/g, respectively.

**2.2. Catalytic Activity of $ZnAl_2O_4$.** SSal was used to be the target pollutant to evaluate the catalytic activity of $ZnAl_2O_4$ samples. The removal of SSal and chemical oxygen demand (COD) was investigated by ozonation degradation of SSal, and the results are presented in Figure 4. Figure 4a showed the efficiency of SSal removal in ozonation and catalytic ozonation with $ZnAl_2O_4$−H. After 60 min, the removal rate of SSal reached 64.8% in catalytic ozonation with $ZnAl_2O_4$−H, while it was only 49.4% in ozonation. Almost no pollutant was adsorbed on the $ZnAl_2O_4$−H surface with the results of adsorption experiments. Figure 4b showed the SSal removal in the presence of different $ZnAl_2O_4$ samples. All the three prepared samples demonstrated good catalytic activity for degradation SSal. The removal rate of SSal was 59 and 61.7% in catalytic ozonation for $ZnAl_2O_4$−C and $ZnAl_2O_4$−S, respectively.

Figure 4c shows the results of COD removal using various $ZnAl_2O_4$ samples. It could be found that the COD was removed only by 33.2% with ozonation after 60 min, while it reached 36.6, 38.8, and 46.2% in the presence of $ZnAl_2O_4$−C, $ZnAl_2O_4$−S, and $ZnAl_2O_4$−H, respectively. On the basis of kinetic analysis, it was found that the results of COD removal were followed the pseudo-first order reaction.[11] When $ZnAl_2O_4$−H was added, the pseudo first-order rate constants increased from $6.3 \times 10^{-3}$ to $10.4 \times 10^{-3}$ $min^{-1}$ compared with ozonation (inset in Figure 4c). The results demonstrated that $ZnAl_2O_4$ displayed a good catalytic performance compared to ozonation for the degradation of SSal. Moreover, the effect of $ZnAl_2O_4$−H was better than $ZnAl_2O_4$−C and $ZnAl_2O_4$−S for both the removal of SSal and COD. According to the characterization results of $ZnAl_2O_4$ with the surface properties, it was found that the catalytic activity of $ZnAl_2O_4$ was positively related to the density of surface hydroxyl groups. Therefore, surface hydroxyl groups would be the critical factor to investigate active oxidative species in catalytic ozonation.

**2.3. Investigation of Active Oxidative Species.** The active oxidative species played an important part in the catalytic ozonation of SSal with $ZnAl_2O_4$, which enhanced the SSal removal and mineralization of organics. On the basis of the reaction mechanism of heterogeneous catalytic ozonation,[10] a stronger hydroxyl radical scavenger of *tert*-butyl alcohol (TBA, 50 mmol/L) was used to verify the formation of $^{\bullet}OH$ because of aqueous ozone decomposition in the presence of $ZnAl_2O_4$ and participated in the reaction with catalytic ozonation.[24] TBA reacted with $^{\bullet}OH$ rapidly and suppressed the chain reaction.[25] Figure 5 shows that the removal rate of SSal was decreased greatly in the ozonation/$ZnAl_2O_4$ when TBA was added. The result indicated that more $^{\bullet}OH$ was formed in the presence of $ZnAl_2O_4$, and it played a crucial role as the active oxidative species for degradation of SSal.



DOI: 10.1021/acsomega.8b00263
ACS Omega 2018, 3, 6506−6512

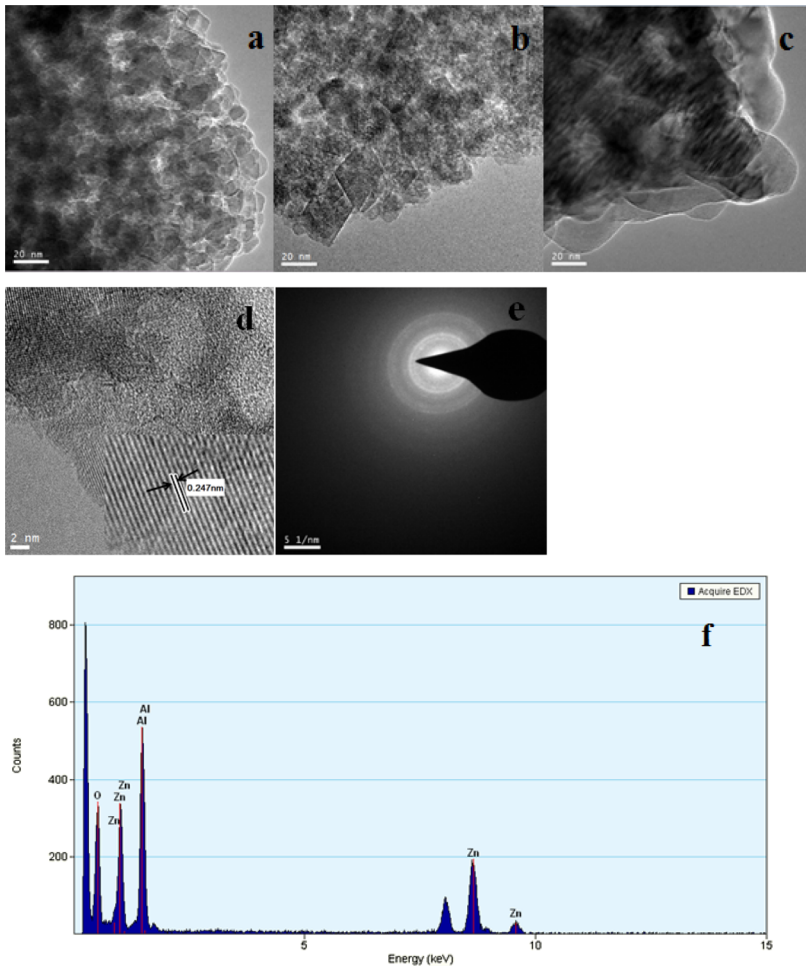


**Figure 2.** TEM micrographs of $ZnAl_2O_4$ samples: (a) $ZnAl_2O_4$–C; (b) $ZnAl_2O_4$–H; (c) $ZnAl_2O_4$–S; (d) high-resolution TEM micrograph of $ZnAl_2O_4$–H; (e) SAED pattern of $ZnAl_2O_4$–H; and (f) EDX pattern of $ZnAl_2O_4$–H.

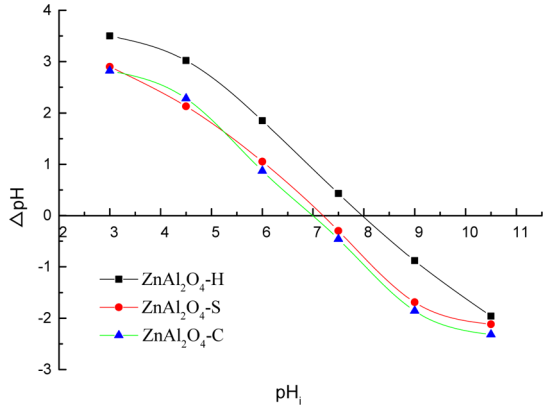


**Figure 3.** $pH_{pzc}$ of $ZnAl_2O_4$ samples.

Figure 6 shows the FT-IR spectra of the synthesis of $ZnAl_2O_4$ by the three methods. FT-IR is an appropriate technique to investigate the chemical adsorption or interaction.[26] The band could be seen at around 3451 $cm^{-1}$ corresponding to the stretching vibrations of −OH groups, which was contributed by the coordinated water.[27,28] As the −OH group's peak of $ZnAl_2O_4$ prepared by the hydrothermal method ($ZnAl_2O_4$–H) was stronger than the other two, which indicated that the $ZnAl_2O_4$–H had a higher density of surface −OH groups. The band at around 1632 $cm^{-1}$ was present in all the samples, which could be assigned to the H−O−H bending vibrations of the adsorbed water molecule. The band at 1382 $cm^{-1}$ was presented in the $ZnAl_2O_4$–H alone, which was the OH group in the metal alkoxides.[29] In all the samples, the bands at around 666, 558, and 506 $cm^{-1}$ were assigned to stretching and bending modes of the Al single bond O of octahedral $AlO_6$ units; this suggested that the normal spinel-type $ZnAl_2O_4$ structure was formed.

The chemical composition and relative content of the surface element for environmental material are important to the effects in application of wastewater treatment.[30−32] Therefore, XPS analysis was carried out to explore the characteristics of the $ZnAl_2O_4$ surface (Figure 7). The wide XPS spectra of $ZnAl_2O_4$ contained elements of Zn, Al, O, and C (Figure 7a), in which the presence of the carbon C 1s peak at 284.6 eV was mainly used to calibrate the binding energies of other elements. Figure 7b−d presents the O 1s spectra of the three catalysts with high resolution. In addition, they were fitted by Gauss−Lorentzian peak shapes with the nonlinear least-squares fit program. The results displayed three peaks with binding energies at about 530.0, 531.1, and 532.5 eV. The signal at 530.0 eV possibly comes from $AlO_x$ ($O_{site1}$, Al in the $AlO_6$ octahedral site or $AlO_4$ tetrahedral site).[33] The peak at 531.1 eV can be ascribed to lattice oxygen ($O_{site2}$) in the $ZnAl_2O_4$ crystal lattice.[34] Notably, the peak at 532.5 eV was assigned to surface-adsorptive hydroxyl oxygen species ($O_{site3}$). The relative content of $O_{site3}$



DOI: 10.1021/acsomega.8b00263
ACS Omega 2018, 3, 6506−6512

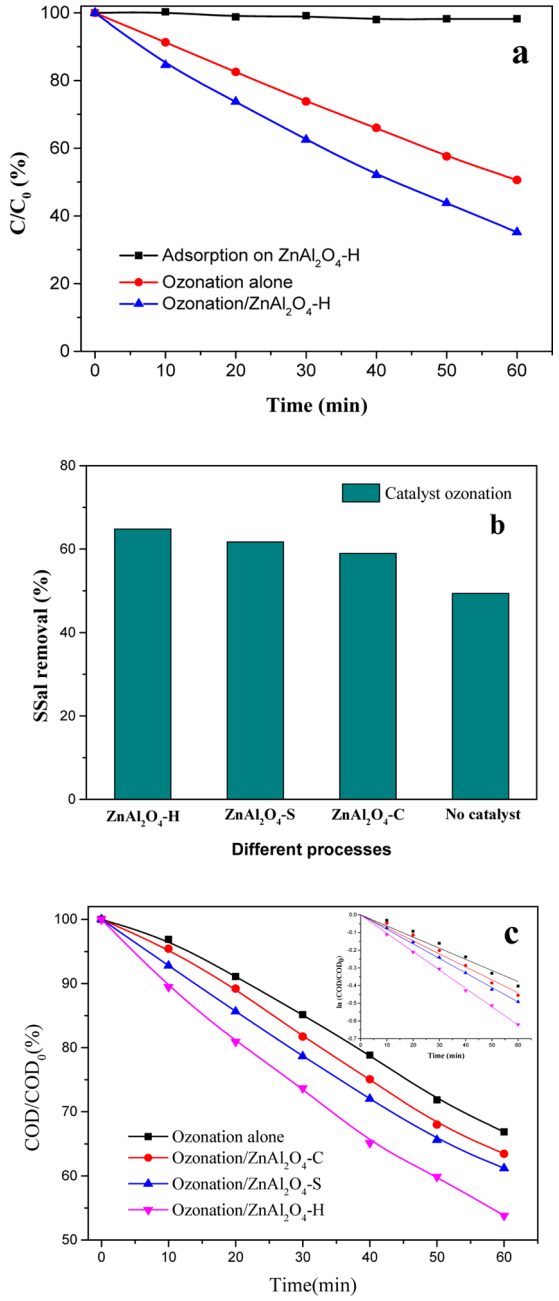


**Figure 4.** SSal degradation efficiency with different processes (a) and with different catalyst samples (b), COD removal rate with different catalyst samples and the insertion shows the fitting results (c). Experimental conditions: initial SSal concentration: 500 mg/L, initial pH = 7.0, ozone dose: 5.0 mg/min (a,b) and 10.0 mg/min (c), catalyst dose: 0.2 g/L.

of catalyst samples can be calculated by the fitted peak area presented in Table 1.[30] It was shown that the percentage of $O_{site3}$ for $ZnAl_2O_4$−H was 11.57%, which was higher than those of $ZnAl_2O_4$−S (8.6%) and $ZnAl_2O_4$−C (8.18%). Also, the $O_{site3}$ is taken as the initiators for •OH generation,[35] and it plays an important role in the ozonation process. Thus, the analysis of XPS demonstrated that •OH could be the active oxidative species in the presence of $ZnAl_2O_4$. Furthermore, the $ZnAl_2O_4$−H which possesses the most percentage of $O_{site3}$ has a better catalytic activity.

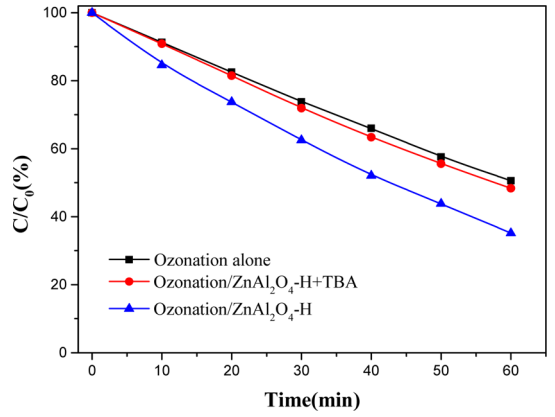


**Figure 5.** Effect of radical scavenger TBA on catalytic ozonation of SSal.

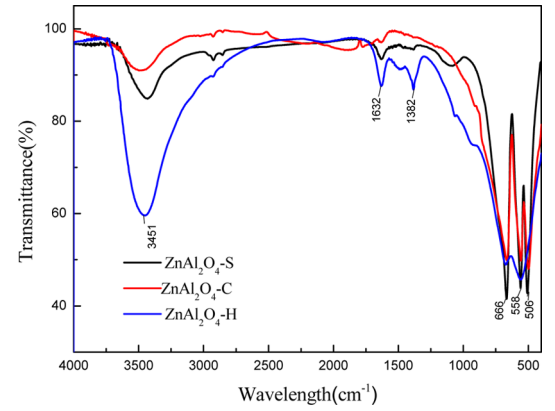


**Figure 6.** FT-IR patterns of $ZnAl_2O_4$ samples.

**2.4. Catalyst Reusability.** The reusability of the catalyst is an important parameter for the consideration of practice application in the future.[36] To investigate the reusability of catalyst samples, a specific experiment was carried out to recycle the $ZnAl_2O_4$−H three times under identical conditions. The catalyst particles were separated with reaction solution by sediment and centrifugation, and then they can be collected for a new cycle. As shown in Figure 8, the removal efficiency of SSal was found to be 64.8−59.7% after being reused three times of catalyst, which indicated that the catalytic activity of $ZnAl_2O_4$−H was not significantly changed after cycling. The results suggested the high reusability and stability of $ZnAl_2O_4$ catalysts in the water treatment.

## 3. CONCLUSIONS

In this paper, nanocrystalline $ZnAl_2O_4$ was prepared by hydrothermal, sol−gel, and coprecipitation methods. In addition, the catalysts were applied in ozonation for the degradation of pollutants. In the presence of three catalyst samples, the degradation of SSal was significantly enhanced compared to ozonation alone. Furthermore, the $ZnAl_2O_4$−H which was prepared by the hydrothermal method possessed the simplest operation with one step and displayed better catalytic activity in catalytic ozonation. Notably, some characterizations of $ZnAl_2O_4$, such as FT-IR and XPS, indicated that the surface of hydroxyl groups was the key during the degradation experiments. In addition, surface hydroxyl groups of the catalyst were regarded as the active sites for the generation of •OH. Accordingly, the experiment of adding TBA was done,



DOI: 10.1021/acsomega.8b00263
ACS Omega 2018, 3, 6506−6512

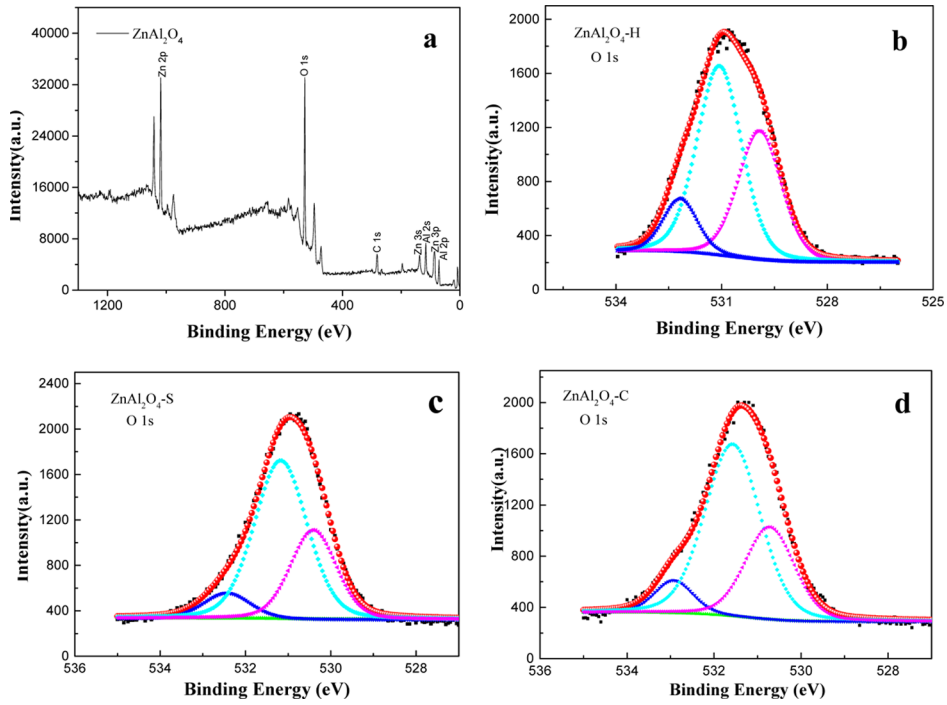


**Figure 7.** Representative XPS characterization of $ZnAl_2O_4$ samples, wide spectrum (a); O 1s spectrum (b–d).

**Table 1. Gaussian Fitting XPS Results of $O_{site3}$ for Catalyst Samples**

| fitting parameter | $ZnAl_2O_4$–H | $ZnAl_2O_4$–S | $ZnAl_2O_4$–C |
|---|---|---|---|
| B.E (eV) | 532.37 | 532.43 | 532.5 |
| area | 530 | 332 | 310 |
| rel. content (%) | 11.57 | 8.60 | 8.18 |

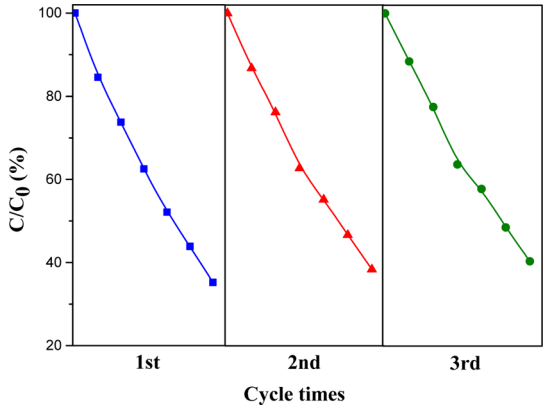


**Figure 8.** Degradation efficiency of SSal by $ZnAl_2O_4$–H for three times in ozonation.

which demonstrated that •OH was the active oxidative species in catalytic ozonation with $ZnAl_2O_4$. On the other hand, $ZnAl_2O_4$–H showed good recyclability by reusing the catalyst samples. This study could provide a method for novel catalyst preparation and determine the potentially promising applications of $ZnAl_2O_4$ in catalytic ozonation of wastewater treatment.

## 4. EXPERIMENTAL SECTION

**4.1. Chemicals.** SSal was selected as the model pollutant, and it was obtained from J&K scientific Co., Ltd. Zinc nitrate hexahydrate [$Zn(NO_3)_2{\cdot}6H_2O$] and aluminum nitrate nonahydrate [$Al(NO_3)_3{\cdot}9H_2O$] were purchased from Aladdin Reagent (China) Co., Ltd. Ammonium iron sulfate dodecahydrate [$(NH_4)\ Fe(SO_4)_2{\cdot}12H_2O$] was purchased from Shanghai Macklin Chemical Reagent (China) Co., Ltd. TBA was chosen as the radical scavenger and purchased from Nanjing Chemical Reagent (China) Co., Ltd. The urea was obtained from Sinopharm Chemical Reagent Co., Ltd. Other reagents used in the work were of analytical grade. Ultrapure water was used in the research from Mili-Q water (18.2 MΩ cm in resistivity).

**4.2. Preparation of $ZnAl_2O_4$.** Three nanocrystalline $ZnAl_2O_4$ catalysts were synthesized by hydrothermal, sol–gel, and coprecipitation methods.

*Hydrothermal Method.* $Zn(NO_3)_2{\cdot}6H_2O$ (8 mmol), $Al(NO_3)_3{\cdot}9H_2O$ (16 mmol), and urea (0.16 mol) were added into a 160 mL of mixture solvent of water and ethanol (v/v = 1:1) with magnetic stirring. After dissolving completely, the clear solution was transferred into a 200 mL Teflon-lined stainless autoclave and heated at 180 °C for 24 h. When it cooled to room temperature, the supernatant catalyst was filtered by centrifugation, and then it was washed with ethanol and ultrapure water until the pH value got to neutral. The obtained catalyst was dried at 80 °C and denoted as $ZnAl_2O_4$–H.

*Sol–Gel Method.* $Zn(NO_3)_2{\cdot}6H_2O$ (8 mmol) and $Al(NO_3)_3{\cdot}9H_2O$ (16 mmol) were dissolved in 80 mL of ultrapure water, and then a mixture of metal nitrate (M1) was obtained. Then, the citric acid was dissolved in ultrapure water (M2), with the molar ratio of citric acid and the metal ions being 2:1. Then, M1 was added dropwise into M2 while stirring continuously. After 10 min of stirring, the solution was heated at 70 °C in a water bath until the sols were formed. The transparent thick gels were formed and then maintained at 150 °C for 2 h to obtain a fluffy polyporous powder. After grinding, the abovementioned powder was calcined at 700 °C for 8 h in



DOI: 10.1021/acsomega.8b00263
ACS Omega 2018, 3, 6506–6512

the muffle furnace and then annealed at 400 °C for 3 h; it is denoted as $ZnAl_2O_4$−S.[37]

*Coprecipitation Method.* $Zn(NO_3)_2{\cdot}6H_2O$ (8 mmol) and $Al(NO_3)_3{\cdot}9H_2O$ (16 mmol) were dissolved in 10 mL of ultrapure water, wherein the molar ratio of Zn/Al was 1:2, and the two solutions were mixed sufficiently. Then, the aqueous ammonia solution (25 wt %) was dropped into the above-mentioned solution, and the mixture was stirred fully until complete precipitation. The precipitate was filtered by centrifugation, washed with deionized water and ethanol, and dried at 80 °C. Then, the dry product was calcined at 700 °C for 8 h and denoted as $ZnAl_2O_4$−C.

**4.3. Characterization of $ZnAl_2O_4$.** The composition and phase of samples were determined by XRD with Cu K$\alpha$ radiating (Rigaku D/MAX 2500 PC) under the condition of 40 kV voltage, 300 mA tube current, and continuous scan mode sampling. The scan speed was 4° $min^{-1}$ with a range of 10°−90°. The morphologies and size of catalysts were characterized by TEM. For preparing the samples of TEM, the powder of the catalyst need to be dispersed by ethanol and then drops of each samples placed on a copper grid. Element composition of samples was investigated by EDX. The FT-IR spectrum was recorded on a Nicolet Magna-IR 6700 infrared spectrometer. The XPS was analyzed using a PHI5700 spectrometer.

The density of surface hydroxyl groups of catalysts was measured by a saturated deprotonating method.[38] The procedure was as follows: 0.3 g of $ZnAl_2O_4$ was added to 50 mL of 2−100 mmol/L NaOH solution, and the suspensions were shaken at 25 °C for 24 h.

The pH at the point of zero charge ($pH_{pzc}$) of catalysts was determined by a pH drift method.[39] The 0.1 M NaCl solution was prepared as an electrolyte, and $N_2$ was bubbled through the solution to expel the dissolved $CO_2$. Then, the pH was adjusted to successive initial values by NaOH and $HNO_3$ as $pH_i$. After that, the $ZnAl_2O_4$ (0.1 g) was added to the solution. These suspensions were shaken for 24 h with the temperature at 25 °C. The final pH was measured by a pH meter called $pH_f$ and using the equation of $\Delta pH = pH_f - pH_i$ to calculate a series of $\Delta pH$. $\Delta pH$ was plotted against the initial pH. The pH at which the curve crosses the *X*-axis is taken as the $pH_{pzc}$.

**4.4. Experimental Procedures.** The degradation experimental equipment of SSal consisted of a cylindrical pyrex glass reactor, an ozone generator (CFY-3, Hangzhou Rongxin Electronic Equipment Co., Ltd., China), a mass flowmeter, and an exhaust treatment system. The ozone reactor consists of three parts with inner pipe, outer pipe and pedestal, and an ozone diffuser fixed in the bottom. When the reaction started, as ozone was diffusing, the wastewater and catalyst were flowed circularly between the two pipes, which formed a system of a circulating fluidized bed. The initial concentration of SSal is 500 mg/L, 1.5 L of SSal solution, and 0.30 g of catalyst was added into the reactor, and then ozone was bubbled from the bottom continuously. To test the performance of $ZnAl_2O_4$, other experiments were carried out without the catalyst and absorption on the catalyst under the same condition. In addition, x, the dosage of ozone, was controlled by adjusting the mass flowmeter, the pH of SSal solution was adjusted by HCl and NaOH, and pH was adjusted in 7.0 with ozonation and catalytic ozonation. All the tests were performed three times, and the final results were averaged.

The concentration of SSal was analyzed by adding ferric ion in excess, for SSal can react with the ferric ion to form the colored metal complex of $[Fe(SSal)]^{3+}$, which presents characteristic absorbance at 500 nm.[40] Before measuring, the pH value of samples was adjusted to lower than 2.5 by 0.01 mol/L $HClO_4$. The absorbance of $[Fe(SSal)]^{3+}$ was measured via a Hach UV−vis spectrophotometer (Hach DR6000, USA).

The COD is $COD_{cr}$ and it was analyzed by the fast digestion spectrophotometric method. The samples were digested at 150 °C for 2 h, and the absorbance was determined at 440 nm by the Hach UV−vis spectrophotometer.

## AUTHOR INFORMATION


### Corresponding Authors

*E-mail: dqz99@163.com (Q.D.).

*E-mail: jchen@zjut.edu.cn (J.C.).

### ORCID

Jianmeng Chen: 0000-0001-7752-1072


### Notes

The authors declare no competing financial interest.

## ACKNOWLEDGMENTS

The authors are grateful for the financial support provided by the Basic Public Projects of Zhejiang Province (LGJ18E080001) and National Natural Science Foundation of China (21306175).

## REFERENCES


(1) Pozdnyakov, I. P.; Plyusnin, V. F.; Grivin, V. P.; Vorobyev, D. Y.; Kruppa, A. I.; Lemmetyinen, H. Photochemistry of sulfosalicylic acid in aqueous solutions. *J. Photochem. Photobiol. Chem.* **2004**, *162*, 153.

(2) Sillanpää, M. E. T.; Kurniawan, T. A.; Lo, W.-h. Degradation of chelating agents in aqueous solution using advanced oxidation process (AOP). *Chemosphere* **2011**, *83*, 1443.

(3) Tušar, N. N.; Maučec, D.; Rangus, M.; Arčon, I.; Mazaj, M.; Cotman, M.; Pintar, A.; Kaučič, V. Manganese Functionalized Silicate Nanoparticles as a Fenton-Type Catalyst for Water Purification by Advanced Oxidation Processes (AOP). *Adv. Funct. Mater.* **2012**, *22*, 820.

(4) Weng, M.; Pei, J. Electrochemical oxidation of reverse osmosis concentrate using a novel electrode: Parameter optimization and kinetics study. *Desalination* **2016**, *399*, 21.

(5) Dai, Q.; Zhou, J.; Meng, X.; Feng, D.; Wu, C.; Chen, J. Electrochemical oxidation of cinnamic acid with Mo modified $PbO_2$ electrode: Electrode characterization, kinetics and degradation pathway. *Chem. Eng. J.* **2016**, *289*, 239.

(6) Dai, Q.; Chen, W.; Luo, J.; Luo, X. Abatement kinetics of highly concentrated 1H-Benzotriazole in aqueous solution by ozonation. *Sep. Purif. Technol.* **2017**, *183*, 327.

(7) Weng, M. L.; Zhang, X. J. Optimization for the Degradation of Isonicotinohydrazide by Electrochemical Oxidation. *Int. J. Electrochem. Sci.* **2014**, *9*, 3327.

(8) Weng, M. L.; Zhou, Z. J.; Zhang, Q. Electrochemical Degradation of Typical Dyeing Wastewater in Aqueous Solution: Performance and Mechanism. *Int. J. Electrochem. Sci.* **2013**, *8*, 290.

(9) Dai, Q.; Xia, Y.; Sun, C.; Weng, M.; Chen, J.; Wang, J.; Chen, J. Electrochemical degradation of levodopa with modified $PbO_2$ electrode: Parameter optimization and degradation mechanism. *Chem. Eng. J.* **2014**, *245*, 359.

(10) Dai, Q.; Wang, J.; Yu, J.; Chen, J.; Chen, J. Catalytic ozonation for the degradation of acetylsalicylic acid in aqueous solution by magnetic $CeO_2$ nanometer catalyst particles. *Appl. Catal., B* **2014**, *144*, 686.

(11) Dai, Q.; Chen, L.; Zhou, S.; Chen, J. Kinetics and mechanism study of direct ozonation organics in aqueous solution. *RSC Adv.* **2015**, *5*, 24649.

(12) Nawrocki, J.; Kasprzyk-Hordern, B. The efficiency and mechanisms of catalytic ozonation. *Appl. Catal., B* **2010**, *99*, 27.




DOI: 10.1021/acsomega.8b00263
*ACS Omega* 2018, 3, 6506−6512

(13) Zhao, L.; Sun, Z.; Ma, J. Novel Relationship between Hydroxyl Radical Initiation and Surface Group of Ceramic Honeycomb Supported Metals for the Catalytic Ozonation of Nitrobenzene in Aqueous Solution. *Environ. Sci. Technol.* **2009**, *43*, 4157.
(14) Chen, J.; Wen, W.; Kong, L.; Tian, S.; Ding, F.; Xiong, Y. Magnetically Separable and Durable $MnFe_2O_4$ for Efficient Catalytic Ozonation of Organic Pollutants. *Ind. Eng. Chem. Res.* **2014**, *53*, 6297.
(15) Bing, J.; Hu, C.; Nie, Y.; Yang, M.; Qu, J. Mechanism of catalytic ozonation in $Fe_2O_3/Al_2O_3$@SBA-15 aqueous suspension for destruction of ibuprofen. *Environ. Sci. Technol.* **2015**, *49*, 1690.
(16) Zhao, H.; Dong, Y.; Wang, G.; Jiang, P.; Zhang, J.; Wu, L.; Li, K. Novel magnetically separable nanomaterials for heterogeneous catalytic ozonation of phenol pollutant: $NiFe_2O_4$ and their performances. *Chem. Eng. J.* **2013**, *219*, 295.
(17) Farhadi, S.; Panahandehjoo, S. Spinel-type zinc aluminate ($ZnAl_2O_4$) nanoparticles prepared by the co-precipitation method: A novel, green and recyclable heterogeneous catalyst for the acetylation of amines, alcohols and phenols under solvent-free conditions. *Appl. Catal., A* **2010**, *382*, 293.
(18) Iaiche, S.; Djelloul, A. $ZnO/ZnAl_2O_4$ Nanocomposite Films Studied by X-Ray Diffraction, FTIR, and X-Ray Photoelectron Spectroscopy. *J. Spectrosc.* **2015**, *2015*, 1.
(19) Zawadzki, M.; Staszak, W.; López-Suárez, F. E.; Illán-Gómez, M. J.; Bueno-López, A. Preparation, characterisation and catalytic performance for soot oxidation of copper-containing $ZnAl_2O_4$ spinels. *Appl. Catal., A* **2009**, *371*, 92.
(20) Freeda, M.; Suresh, G. Structural and Luminescent properties of Eu-doped $CaAl_2O_4$ Nanophosphor by sol-gel method. *Mater. Today Proc.* **2017**, *4*, 4260.
(21) Walerczyk, W.; Zawadzki, M. Structural and catalytic properties of $Pt/ZnAl_2O_4$ as catalyst for VOC total oxidation. *Catal. Today* **2011**, *176*, 159.
(22) Wang, C.-H.; Hsu, H.-C.; Hu, J.-H. High-energy asymmetric supercapacitor based on petal-shaped $MnO_2$ nanosheet and carbon nanotube-embedded polyacrylonitrile-based carbon nanofiber working at 2 V in aqueous neutral electrolyte. *J. Power Sources* **2014**, *249*, 1.
(23) Zhang, T.; Li, C.; Ma, J.; Tian, H.; Qiang, Z. Surface hydroxyl groups of synthetic $\alpha$-FeOOH in promoting •OH generation from aqueous ozone: Property and activity relationship. *Appl. Catal., B* **2008**, *82*, 131.
(24) Valdés, H.; Zaror, C. A. Heterogeneous and homogeneous catalytic ozonation of benzothiazole promoted by activated carbon: kinetic approach. *Chemosphere* **2006**, *65*, 1131.
(25) Acero, J. L.; Stemmler, K.; Gunten, U. V. Degradation Kinetics of Atrazine and Its Degradation Products with Ozone and •OH Radicals: A Predictive Tool for Drinking Water Treatment. *Environ. Sci. Technol.* **2000**, *34*, 591.
(26) Wang, L.; Sun, Y.; Wang, J.; Wang, J.; Yu, A.; Zhang, H.; Song, D. Preparation of surface plasmon resonance biosensor based on magnetic core/shell $Fe_3O_4/SiO_2$ and $Fe_3O_4/Ag/SiO_2$ nanoparticles. *Colloids Surf., B* **2011**, *84*, 484.
(27) Ballarini, A. D.; Bocanegra, S. A.; Castro, A. A.; de Miguel, S. R.; Scelza, O. A. Characterization of $ZnAl_2O_4$ Obtained by Different Methods and Used as Catalytic Support of Pt. *Catal. Lett.* **2009**, *129*, 293.
(28) Ge, D.-L.; Fan, Y.-J.; Qi, C.-L.; Sun, Z.-X. Facile synthesis of highly thermostable mesoporous $ZnAl_2O_4$ with adjustable pore size. *J. Mater. Chem. A* **2013**, *1*, 1651.
(29) Motloung, S. V.; Dejene, F. B.; Swart, H. C.; Ntwaeaborwa, O. M. Effects of $Pb^{2+}$ ions concentration on the structure and PL intensity of Pb-doped $ZnAl_2O_4$ nanocrystals synthesized using sol−gel process. *J. Sol-Gel Sci. Technol.* **2014**, *70*, 422.
(30) Dai, Q.; Xia, Y.; Chen, J. Mechanism of enhanced electrochemical degradation of highly concentrated aspirin wastewater using a rare earth La-Y co-doped $PbO_2$ electrode. *Electrochim. Acta* **2016**, *188*, 871.
(31) Dai, Q.; Chen, L.; Chen, W.; Chen, J. Degradation and kinetics of phenoxyacetic acid in aqueous solution by ozonation. *Sep. Purif. Technol.* **2015**, *142*, 287.
(32) Dai, Q.; Zhou, J.; Weng, M.; Luo, X.; Feng, D.; Chen, J. Electrochemical oxidation metronidazole with Co modified $PbO_2$ electrode: Degradation and mechanism. *Sep. Purif. Technol.* **2016**, *166*, 109.
(33) Pitale, S. S.; Kumar, V.; Nagpure, I. M.; Ntwaeaborwa, O. M.; Swart, H. C. Luminescence characterization and electron beam induced chemical changes on the surface of $ZnAl_2O_4$:Mn nanocrystalline phosphor. *Appl. Surf. Sci.* **2011**, *257*, 3298.
(34) Strohmeier, B. R. Zinc Aluminate ($ZnAl_2O_4$) by XPS. *Surf. Sci. Spectra* **1994**, *3*, 128.
(35) Zhang, F.; Wei, C.; Hu, Y.; Wu, H. Zinc ferrite catalysts for ozonation of aqueous organic contaminants: phenol and bio-treated coking wastewater. *Sep. Purif. Technol.* **2015**, *156*, 625.
(36) Zou, R.; Wen, S.; Zhang, L.; Liu, L.; Yue, D. Preparation of Rh−$SiO_2$ fiber catalyst with superioractivity and reusability by electrospinning. *RSC Adv.* **2015**, *5*, 99884.
(37) Chen, L.; Sun, X.; Liu, Y.; Zhou, K.; Li, Y. Porous $ZnAl_2O_4$ synthesized by a modified citrate technique. *J. Alloys Compd.* **2004**, *376*, 257.
(38) Tamura, H.; Tanaka, A.; Mita, K.-y.; Furuichi, R. Surface Hydroxyl Site Densities on Metal Oxides as a Measure for the Ion-Exchange Capacity. *J. Colloid Interface Sci.* **1999**, *209*, 225.
(39) Aldegs, Y.; Elbarghouthi, M.; Elsheikh, A.; Walker, G. Effect of solution pH, ionic strength, and temperature on adsorption behavior of reactive dyes on activated carbon. *Dyes Pigm.* **2008**, *77*, 16.
(40) Liu, H.; Cheng, S.; Zhang, J.; Cao, C. Titanium dioxide as photocatalyst on porous nickel: adsorption and the photocatalytic degradation of sulfosalicylic acid. *Chemosphere* **1999**, *38*, 283.



DOI: 10.1021/acsomega.8b00263
*ACS Omega* 2018, 3, 6506−6512